doi:10.3788/gzxb20184702.0230001

基于 DOAS 及统计量的低浓度 SO_2 测量方法

张豹,高潮,郭永彩,刘国庆,陈方

(重庆大学 光电工程学院 光电技术及系统教育部重点实验室,重庆 400044)

摘 要:为监测燃煤电厂低浓度 SO_2 排放,达到国家超低排放标准,提出一种短光程下测量低浓度 SO_2 的方法.在已知温度压强条件下,利用差分吸收光谱法,由不同浓度的标准气体构建 SO_2 差分吸收截面数据集;根据数据集标准差及均值,结合浓度反演结果,将测量区间由 200~400 nm 逐步缩小到 294~308 nm.对该区间内 137 个波长采样点,用统计学方法,借助标准差及均值表征差分吸收截面精度,同时剔除误差较大的采样点,得到该环境下最优采样点集和差分吸收截面最优数据集.在同等温度压强条件下,利用该最优数据集和差分吸收光谱法,能够以较高精度计算出烟气中 SO_2 浓度.实验采用 420 cm 光程,气室容积 0.5 L,气室内温度 299.05 K,压强 101.33 kPa,测量范围 2~30 μL/L.实验结果表明该方法相对误差低于 1.7%,满量程误差低于 1.3%,零漂 0.09 μL/L,72 h 内重复性良好.在 420 cm 光程条件下,该方法能够高精度测量 30 μL/L 内的 SO_2 气体,解决差分吸收光谱法中浓度与光程之间的冲突,适用于燃煤电厂超低排放监测仪器的研制.

关键词:大气光学;气体监测系统;统计量;二氧化硫;吸收光谱;烟气;差分光学吸收光谱

中图分类号:X831;O433.4;O433.5+1 **文献标识码**:A **文章编号**:1004-4213(2018)02-0230001-8

Measurement Method for Low-concentration SO_2 Based on Statistics and DOAS

ZHANG Bao, GAO Chao, GUO Yong-cai, LIU Guo-qing, CHEN Fang

(*Key Laboratory of Optoelectronic Technology and Systems of Ministry of Education, School of Optoelectronic Engineering, Chongqing University, Chongqing* 400044, *China*)

Abstract: In order to monitor SO_2 emission from coal-fired power factories and meet national ultra-low emission standards, measurement method for low-concentration SO_2 via short optical length is proposed. At known pressure and temperature conditions, dataset of differential absorption cross section was constructed with various concentrations of standard gas, utilizing differential optical absorption spectroscopy (DOAS). In accordance with standard deviation and average of the dataset, combined with results of concentration inversion, spectral window was gradually reduced from 200~400 nm to 294~308 nm. For each point in 294~308 nm, where there are 137 sampling points, statistics and standard deviation were applied to characterize consistency of differential absorption cross section. It was only when standard deviation and average at sampling point met requirements that the point was reserved to optimal point set. So optimal dataset of differential absorption cross section and optimal sampling points were constructed eventually. At same pressure and temperature conditions, SO_2 concentration in flue gases can be accurately calculated by the optimal dataset and DOAS. In the laboratory, measurement range is 2~30 μL/L, temperature and pressure are 299.05 K, 101.33 kPa, while optical length and volume of gas cell are 420 cm, 0.5 L correspondingly. Experimental results show that inversion concentration performs superior repeatability within 72 h, relative error is less than 1.7%, full scale error is below 1.3%, and zero drift is 0.09 μL/L. With 420 cm optical length, the method can precisely

Foundation item: National Key Research and Development Program of China (No. 2016YFF0102802)

First author: ZHANG Bao (1990-), male, M.S. degree, mainly focuses on environmental monitoring and trace gas measurement. Email: zhangbao@cqu.edu.cn

Supervisor: GAO Chao (1959-), male, professor, Ph.D. degree, mainly focuses on environmental monitoring, precision instrument design and so on. Email: gaoc@cqu.edu.cn

Contact author: GUO Yong-cai (1963-), female, professor, Ph.D. degree, mainly focuses on environmental monitoring, light scattering theory and so on. Email: ycguo@cqu.edu.cn

Received: Jul.11, 2017; **Accepted**: Nov.7, 2017

measure low-concentration SO_2 under 30 μL/L, resolve conflicts between concentration and optical length, which is suitable for study of ultra-low emission monitoring system used in coal-fired power plants.

Key words: Atmospheric optics; Gas detectors; Statistics; Sulfur dioxide; Absorption spectroscopy; Flue gases; Differential optical absorption spectroscopy

OCIS Codes: 010.1120; 300.1030; 300.6170; 300.6540; 200.4560

0 Introduction

Coal-fired power plants, emitting contaminants such as NO_2 and SO_2 which seriously affect human health and environment[1], are main form of Chinese power stations. In order to achieve green development, ultra-low emission policies have been issued by Chinese government and restrict SO_2 emission standard to 30 μL/L (at 299.05 K, 101.33 kPa). Therefore, measurement range of SO_2 monitor must be restricted to 30 μL/L or less, while optical length of gas cell must be short enough considering system integration.

DOAS algorithm is widely applied in SO_2 measurement, by the linear relationship between differential optical density and differential absorption cross section. With zenith-sky mobile DOAS measurements, Constantin et al[2]. observed SO_2 and NO_2 vertical column density. Utilizing modeled Fraunhofer reference spectrum and automated DOAS networks, Luebcke et al[3]. retrieved SO_2 column amounts. Automatic plume segmentation was also applied in the field by Osorio et al[4], while gas imaging techniques were adopted in imaging DOAS by Platt et al[5]. Installed measurement instruments at about 5 m above the ground, Bouebdelli et al[6]. researched pollutants concentrations variability. By means of broadband absorption spectroscopy in wavelength range 198～222 nm, Wang et al[7]. designed a highly sensitive detection for SO_2. Temporal variation and vertical distribution of SO_2 were characterized by Wang et al[8]. based on multi-axis differential optical absorption spectroscopy.

For SO_2 monitor designed on active DOAS, lower limit and high precision are accompanied by long optical length, which is not conducive to industrial production and instrument integration. Moreover, considering repeatability and adaptability, the paper proposes a novel method via DOAS and statistics, to resolve the conflicts between measurement limit and optical length. For the reason that differential absorption characteristics change dramatically with temperature and pressure[8-9], the method constructed dataset of absorption cross section varying with environment, which was adopted to retrieve SO_2 concentration in corresponding environment. Different spectral windows for concentration retrieval produce different accuracy[10-11], so the optimal spectral window we used was determined by statistics. In the study, temperature and pressure are 299.05 K, 101.33 kPa correspondingly. Optimal dataset of absorption cross section and sampling points were constructed in proper spectral window (294～308 nm). Experimental results show that the optimal dataset can measure low-concentration SO_2 under 30 μL/L with improved accuracy, and resolve conflicts between optical length and lower limit.

1 Basic theory of DOAS

As shown in Fig. 1, a beam of incident light whose intensity is $I_o(\lambda_i)$, passes through gas cell containing SO_2. Transmitted intensity expressed as $I(\lambda_i)$ is measured by spectrometer. Taking into account Rayleigh scattering, Mie scattering, instrument error and turbulence etc.[12], mathematical model is expressed as[13]

$$I(\lambda_i)=I_o(\lambda_i)\cdot\exp\left[-L\cdot(\sigma(\lambda_i)\cdot c+\varepsilon_R(\lambda_i)+\varepsilon_M(\lambda_i))\right]\cdot A(\lambda_i) \tag{1}$$

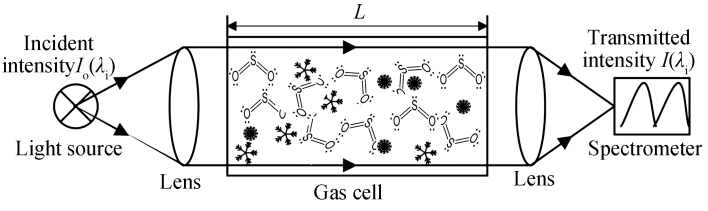

Fig.1 Schematic diagram of DOAS

where, λ_i denotes sampling point of wavelength; L is optical length (cm); and c is concentration of SO_2 (molecule/cm^3); $\sigma(\lambda_i)$ denotes absorption cross section (cm^2/molecule); $\varepsilon_R(\lambda_i)$ and $\varepsilon_M(\lambda_i)$ are Rayleigh and Mie extinction coefficient respectively; $A(\lambda_i)$ is attenuation factor of system[14].

According to gas absorption characteristics, $\sigma(\lambda_i)$ is separated into two parts.

$$\sigma(\lambda_i)=\sigma_{slow}(\lambda_i)+\sigma'(\lambda_i) \tag{2}$$

where, $\sigma_{slow}(\lambda_i)$ varies slowly with wavelength due to Rayleigh scattering, Mie scattering and all broad band absorption; $\sigma'(\lambda_i)$ represents differential absorption cross section which varies rapidly with wavelength.

Combined with Eq.(2), Eq.(1) can be modified as

$$I(\lambda_i)=I_o(\lambda_i)\cdot\exp[-L\cdot\sigma'(\lambda_i)\cdot c]\cdot\exp[-L\cdot(\sigma_{slow}(\lambda_i)\cdot c+\varepsilon_R(\lambda_i)+\varepsilon_M(\lambda_i))]\cdot A(\lambda_i) \tag{3}$$

$$I_o'(\lambda_i)=I_o(\lambda_i)\cdot\exp[-L\cdot(\sigma_{slow}(\lambda_i)\cdot c+\varepsilon_R(\lambda_i)+\varepsilon_M(\lambda_i))]\cdot A(\lambda_i) \tag{4}$$

where, $I_o'(\lambda_i)$ is caused by extinction, turbulence and all broad band absorption structures, and is acquired by fifth order polynomial of $I(\lambda_i)$ in our study.

Eqs.(3) (4) can be rearranged as

$$\mathrm{OD}'(\lambda_i)=\ln\frac{I_o'(\lambda_i)}{I(\lambda_i)}=L\cdot\sigma'(\lambda_i)\cdot c \tag{5}$$

$$c=\mathrm{OD}'(\lambda_i)/[L\cdot\sigma'(\lambda_i)] \tag{6}$$

where, $\mathrm{OD}'(\lambda_i)$ is differential optical density.

Consequently, in the case where differential absorption cross section has been known, gas concentration can be deduced from $\mathrm{OD}'(\lambda_i)$ by the least-squares method.

2 Fundamental principle of dataset construction

In the laboratory, $\sigma'(\lambda_i)$ is deduced from known concentration by Eq.(5). Then concentration can be derived from $\sigma'(\lambda_i)$ via Eq.(6) in practical application. Thus precision of $\sigma'(\lambda_i)$ directly affects accuracy of retrieval concentration. As the significant procedure of concentration measurement, optimal differential absorption cross section is obtained by statistics in following procedures.

2.1 Optimal spectral window

Within different wavelength ranges, the overall trend of $I(\lambda_i)$ is different. As the fifth order polynomial of $I(\lambda_i)$, $I_o'(\lambda_i)$ is different as well. So different wavelength ranges directly lead to different precision of $\sigma'(\lambda_i)$[10-11]. Our study calculates concentrations in different wavelength ranges, and gradually shrink wavelength ranges by means of statistics until number of sampling points less than 200.

2.2 Optimal dataset

In the suitable spectral window determined by Section 2.1, all the sampling points are adopted to erect original dataset (described as $[\lambda_1\ \lambda_2\ \lambda_3\cdots\lambda_{i-1}\ \lambda_i]$). Then matrix of differential absorption cross section (Table 1), described as $\mathrm{Mat}_m=[\sigma_m'(\lambda_1)\ \sigma_m'(\lambda_2)\ \sigma_m'(\lambda_3)\cdots\sigma_m'(\lambda_{i-1})\ \sigma_m'(\lambda_i)]^T$, is obtained by transmitted intensity $I_m(\lambda_i)$ at concentration c_m ($I_m(\lambda_i)$ represents $I(\lambda_i)$ at c_m).

$\sigma'(\lambda_i)$ is directly affected by temperature and pressure[8-9]. Theoretically, $\sigma'(\lambda_i)$ remains unchanged if environmental conditions remain stable. So all the data of each row in Table 1 should be theoretically equal. That's means $\sigma_1'(\lambda_i)$, $\sigma_2'(\lambda_i)$, $\sigma_3'(\lambda_i)$, $\cdots$, $\sigma_m'(\lambda_i)$ are equivalent at point λ_i. However, experiments find that they are different due to attenuation, fluctuation of light source, and instrument error etc.[15-16]

In order to purify dataset and minimize measurement error, data which has larger fluctuation need to be removed. As shown in Table 1, sampling points λ_i and $\sigma_m'(\lambda_i)$ are reserved to optimal dataset only when $\mathrm{SD}(\lambda_i)\leqslant 4\%\,|\overline{\sigma'(\lambda_i)}|$. 4% is obtained by experiment analysis. Eventually, optimal dataset of differential absorption cross section, which is conducive to concentration retrieval, is constructed.

Table 1 The matrices Mat_1, Mat_2, $Mat_3\cdots Mat_m$ calculated by concentrations c_1, c_2, $c_3\cdots c_m$ correspondingly

Sampling point λi	Mat_1	Mat_2	Mat_3	…	Mat_m	$\overline{\sigma'(\lambda_i)}^{**}$	SD $(\lambda_i)^{***}$
λ_1	$\sigma'_1(\lambda_1)$	$\sigma'_2(\lambda_1)$	$\sigma'_3(\lambda_1)$	…	$\sigma'_m(\lambda_1)$	$\overline{\sigma'(\lambda_1)}$	SD(λ_1)
λ_2	$\sigma'_1(\lambda_2)$	$\sigma'_2(\lambda_2)$	$\sigma'_3(\lambda_2)$	…	$\sigma'_m(\lambda_2)$	$\overline{\sigma'(\lambda_2)}$	SD(λ_2)
λ_3	$\sigma'_1(\lambda_3)$	$\sigma'_2(\lambda_3)$	$\sigma'_3(\lambda_3)$	…	$\sigma'_m(\lambda_3)$	$\overline{\sigma'(\lambda_3)}$	SD(λ_3)
…	…	…	…	…	…	…	…
λ_{i-1}	$\sigma'_1(\lambda_{i-1})$	$\sigma'_2(\lambda_{i-1})$	$\sigma'_3(\lambda_{i-1})$	…	$\sigma'_m(\lambda_{i-1})$	$\overline{\sigma'(\lambda_{i-1})}$	SD(λ_{i-1})
λ_i	$\sigma'_1(\lambda_i)$	$\sigma'_2(\lambda_i)$	$\sigma'_3(\lambda_i)$	…	$\sigma'_m(\lambda_i)^{*}$	$\overline{\sigma'(\lambda_i)}$	SD(λ_i)

$^{*}\sigma'_m(\lambda_i)$ is element of Mat_m at sampling point λ_i and concentration c_m; $^{**}\overline{\sigma'(\lambda_i)}$ denotes average of each row; ***SD(λ_i) is standard deviation of each row. Temperature and pressure in all experiments are consistent.

3 Experimental system and data analysis

3.1 Experimental system

Laboratory equipment used in our study is showed in Fig.2. Wavelength range and power of deuterium lamp are 200～400 nm, 25 W respectively, optical length and volume of gas cell are 420 cm, 0.5 L correspondingly, resolution of spectrometer is 0.12 nm. All the experiments were conducted in same environment (299.05 K, 101.33 kPa). Concentration range was 2～30 μL/L, gradient was 1 μL/L. (Take 13 μL/L, 15 μL/L, 17 μL/L, 19 μL/L for instance, Fig.3, Fig.4, Fig.5 are depicted in following paper.)

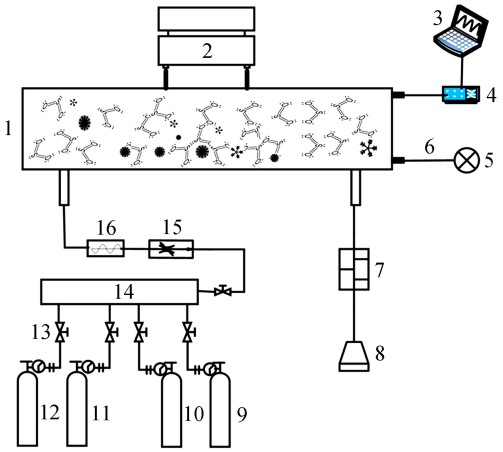

(a) Schematic diagram

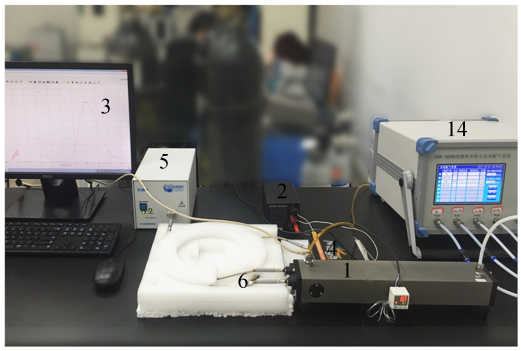

(b) Physical picture

1 gas cell; 2 control system for temperature and pressure; 3 computer; 4 spectrometer; 5 deuterium lamp; 6 optical fiber; 7 purification device for exhaust; 8 exhaust pipe; 9-12 SO_2, NO_2, NO and N_2 standard gas; 13 control valve; 14 gas distribution system; 15 flowmeter; 16 heating belt

Fig.2 Experimental setup

3.2 Data analysis

According to Section 2.2 and Table 1, transmitted intensity $I_m(\lambda_i)$ was obtained at concentration c_m. Thus differential absorption cross section was acquired (Fig.3), where different volatility is presented in different wavelength ranges. By means of preliminary concentration retrieval and theoretical inference[10,17], combined with amplitude and volatility as well, the spectral window 285～318 nm was selected for following analysis (Fig.4). Obviously, compared with Fig.3(c), Fig.4(a) performs superior consistency. In accordance with average value and standard deviation in Fig.4(b), spectral window 285～294 nm was abnegated because of its larger volatility, while spectral window 308～318 nm was also abandoned owing to its lower magnitude. Optimal spectral window 294～308 nm, where there are 137 sampling points via the spectrometer, was acquired finally.

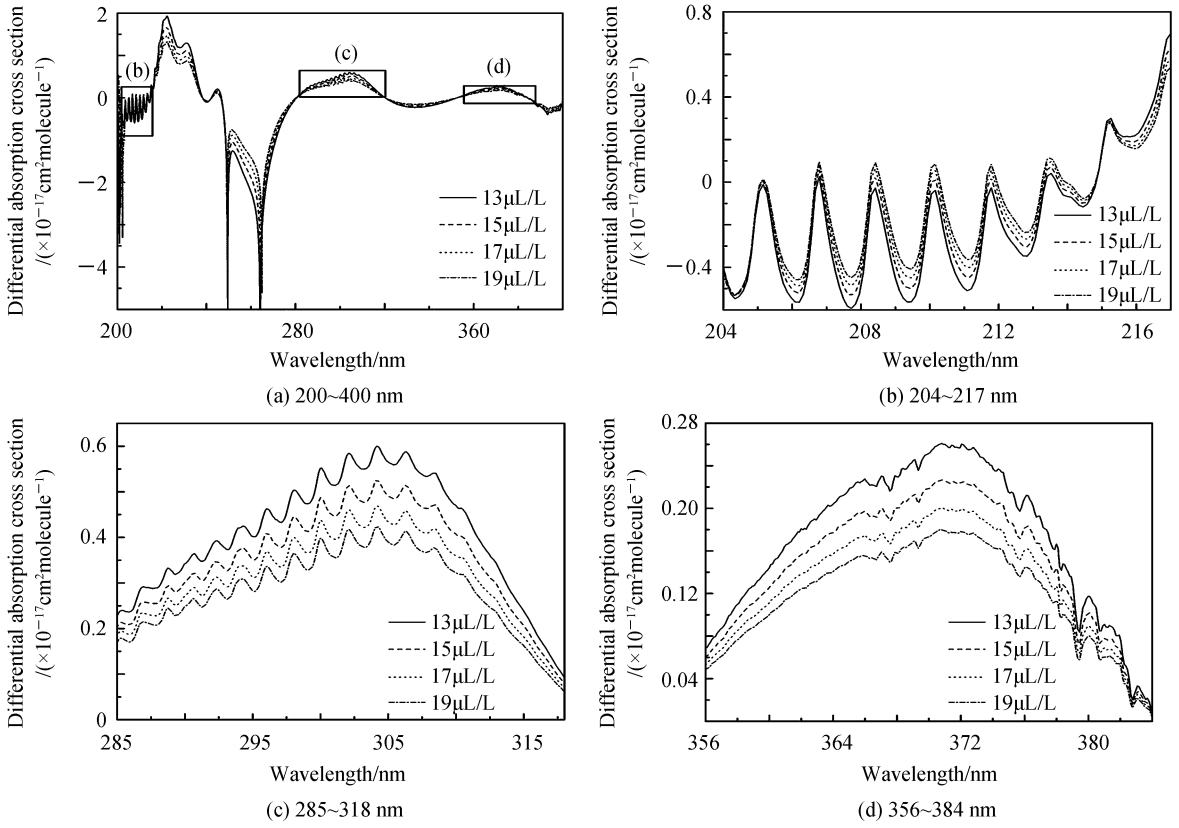

Fig.3 Differential absorption cross section deduced from $I_m(\lambda_i)$ in 200～400 nm

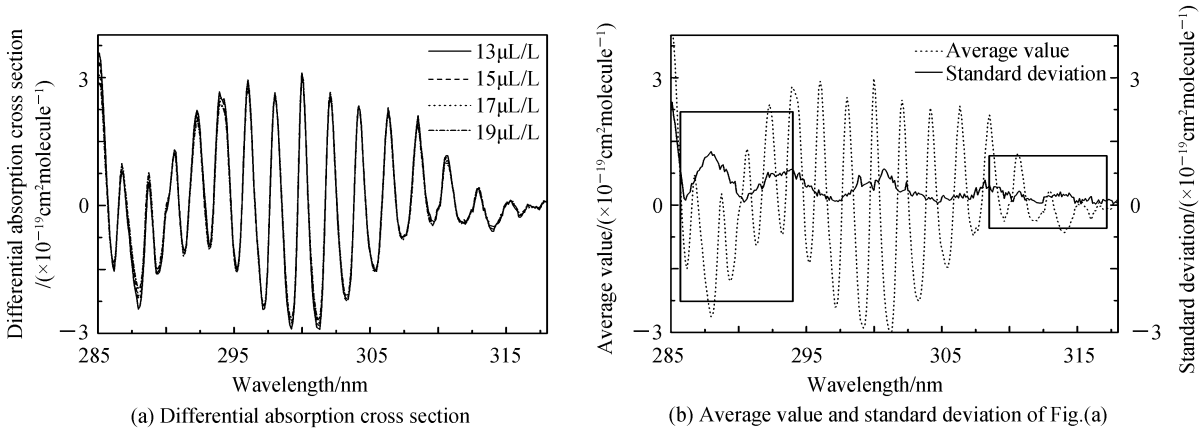

Fig.4 Differential absorption cross section derived from $I_m(\lambda_i)$ in 285～318 nm

As shown in Fig.5, differential absorption cross section in optimal spectral window displays preferable consistency, and standard deviation becomes distinctly smaller. Even now, many unsatisfactory points, especially around peaks, bring unfavorable deviation to concentraton retrieval. Hence the method demonstrated in Section 2.2 was utilized to eliminate sampling points with larger error, and Table 2 was constructed in accordance with Table 1. Optimal sampling points were obtained finally (Fig.6(a)). Thus optimal dataset of differential absorption cross section was acquired for retrieving concentration.

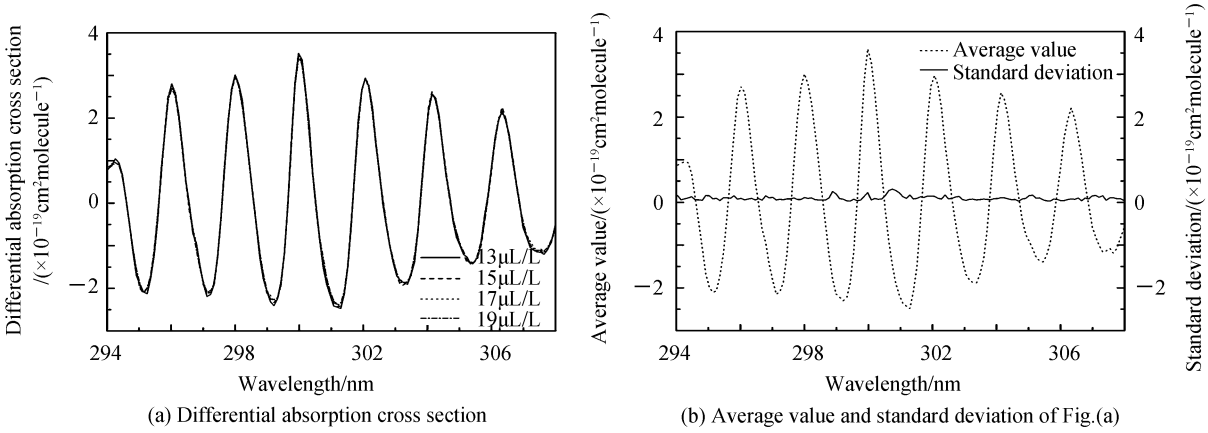

Fig.5 Differential absorption cross section calculated from $I_m(\lambda_i)$ in optimal spectral window 294～308 nm

Table 2 Evaluation of all the sampling points in optimal spectral window based on statistics

Sampling point$_i^{\lambda}$ /nm*	$\lvert\overline{\sigma'(\lambda_i)}\rvert$ of Mat$_m$ /(×10^{-19} cm^2 molecule^{-1})	SD(λ_i) of Mat$_m$ /(×10^{-21} cm^2 molecule^{-1})	SD(λ_i)/$\lvert\overline{\sigma'(\lambda_i)}\rvert$	Extract to optimal dataset**
294.368	0.9347	10.0579	10.761%	NO
297.891	2.6932	6.6924	2.485%	YES
300.088	3.2778	5.5554	1.695%	YES
304.473	1.3384	6.0861	4.547%	NO
306.114	1.5298	4.2583	2.784%	YES
308.299	0.6647	3.8276	5.758%	NO

* There are 137 sampling points in optimal wavelength range 294～308 nm, Table 2 just takes many sampling points for example. ** The optimal point set has 36 optimal sampling points used for deducing optimal differential absorption cross section.

4 Results

Proper spectral window selected in the paper is 294～308 nm, and optimal sampling points in the window is also acquired by statistics and DOAS. According to Section 1, concentration of SO_2 can be calculated by optimal dataset of differential absorption cross section. As shown in Fig.6(b) and Table 3, relative error is less than 1.7%, full scale error is under 1.3%. In many measurement range, relative error can be reduced to 0.8%. Moreover, measurement concentration shows favorable repeatability within 72 h.

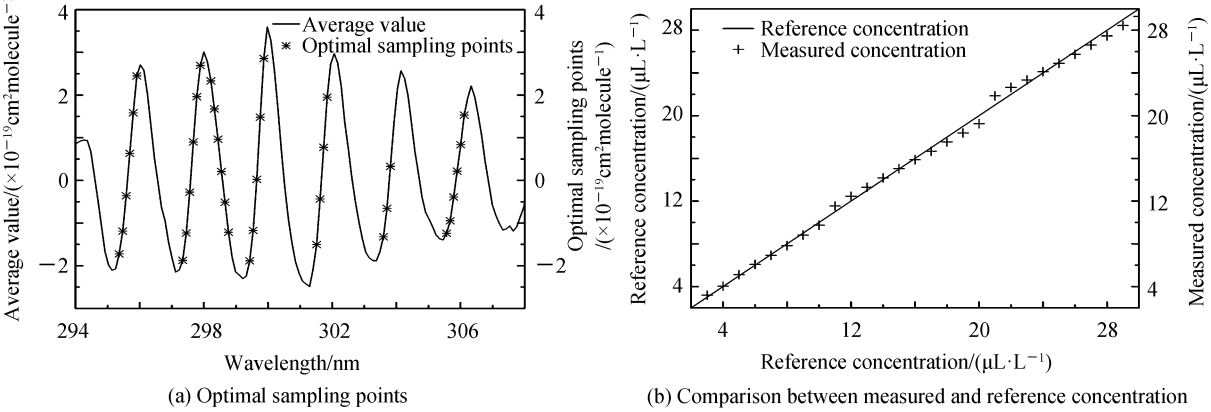

Fig.6 Optimal dataset and measured concentration in the study

Table 3 Measured concentration and relative error in 18th, 19th, 21th of May

Standard concentration /($\mu L \cdot L^{-1}$)	18 May		19 May		21 May	
	Measured concentration /($\mu L \cdot L^{-1}$)	Relative error	Measured concentration /($\mu L \cdot L^{-1}$)	Relative error	Measured concentration/ ($\mu L \cdot L^{-1}$)	Relative error
13	13.08	0.62%	13.04	0.31%	12.94	−0.46%
15	15.02	0.13%	15.03	0.20%	15.07	0.47%
17	16.88	−0.71%	16.9	−0.59%	17.08	0.47%
19	18.74	−1.37%	18.78	−1.16%	18.69	−1.63%

5 Conclusion

A novel measurement method, based on statistics of differential absorption cross section, is demonstrated in the paper. At known pressure and temperature conditions, many experiments were conducted with standard gas. So differential absorption cross section in each known concentration can be calculated via DOAS. According to the theory that absorption cross section is affected dramatically by temperature and pressure, all the cross section we got should be equal theoretically. However, it performs superior consistency in many spectral windows, while has unfavorable volatility in other. Therefore, optimal spectral window was selected by preliminary concentration retrieval. For each sampling point in the range, it was reserved to optimal point set only when it met the condition where $SD(\lambda_i) \leqslant 4\% \left|\overline{\sigma'(\lambda_i)}\right|$. Eventually, dataset of differential absorption cross section, which is applied in concentration retrieval, was obtained at optimal sampling points.

In our study, optical length and volume of gas cell are 420 cm, 0.5 L correspondingly, wavelength range of deuterium lamp is 200～400 nm, and resolution of spectrometer is 0.12 nm. Moreover, all the experiments were conducted at same environment (299.05 K, 101.33 kPa). Optimal wavelength range acquired in the paper are 294～308 nm, while there are 36 optimal sampling points in the range. The relative error measured in the laboratory is less than 1.7%, full scale error is below 1.3%, zero drift is 0.09 μL/L. Meanwhile, measurement results perform superior repeatability in 72 h. With short optical length, lower limit of SO_2 measurement is reduced to 2 μL/L with proper accuracy. According to actual situation of coal-fired power plants, the method is suitable in continuous emission monitoring system. Following research in our team will concentrate on error analysis and enriching numbers of sample, to enhance accuracy and reduce lower limit to 1 μL/L.

References

[1] MORAKINYO O M, ADEBOWALE A S, MOKGOBU M I, *et al*. Health risk of inhalation exposure to sub-10 μm particulate matter and gaseous pollutants in an urban-industrial area in South Africa: An ecological study[J]. *BMJ Open*, 2017, **7**(3): e013941.

[2] CONSTANTIN D E, MERLAUD A, VOICULESCU M, *et al*. NO_2 and SO_2 observations in southeast Europe using mobile DOAS observations[J]. *Carpathian Journal of Earth and Environmental Sciences*, 2017, **12**(2): 323-328.

[3] LUBCKE P, LAMPEL J, ARELLANO S, *et al*. Retrieval of absolute SO_2 column amounts from scattered-light spectra: Implications for the evaluation of data from automated DOAS networks[J]. *Atmospheric Measurement Techniques*, 2016, **9**(12): 5677-5698.

[4] OSORIO M, CASABALLE N, BELSTERLI G, *et al*. Plume segmentation from UV camera images for SO_2 emission rate quantification on cloud days[J]. *Remote Sensing*, 2017, **9**(6):517.

[5] PLATT U, LUBCKE P, KUHN J, *et al*. Quantitative imaging of volcanic plumes - Results, needs, and future trends [J]. *Journal of Volcanology and Geothermal Research*, 2015, **300**(SI): 7-21.

[6] BOUEBDELLI T, BOUCHLAGHEM K, CHOUIKH R, *et al*. Experimental study of pollutants concentrations variability in Tunisia[J]. *European Physical Journal Plus*, 2016, **131**(11):397.

[7] WANG Lin, ZHANG Yun-gang, ZHOU Xue, *et al*. Optical sulfur dioxide sensor based on broadband absorption spectroscopy in the wavelength range of 198～222 nm[J]. *Sensors and Actuators B-Chemical*, 2017, **241**:146-150.

[8] WANG Yang, LAMPEL J, XIE Pin-hua, *et al*. Ground-based MAX-DOAS observations of tropospheric aerosols, NO_2, SO_2 and HCHO in Wuxi, China, from 2011 to 2014[J]. *Atmospheric Chemistry and Physics*, 2017, **17**(3): 2189-2215.

[9] SHI Peng, XIE Pin-hua, QIN Min, *et al*. Cluster analysis for daily patterns of SO_2 and NO_2 measured by the DOAS system in Xiamen[J]. *Aerosol and Air Quality Research*, 2014, **14**(5): 1455-1465.

[10] FICKEL M, GRANADOS H D. On the use of different spectral windows in DOAS evaluations: Effects on the estimation of SO_2 emission rate and mixing ratios during strong emission of Popocatepetl volcano[J]. *Chemical*

Geology, 2017, **462**: 67-73.

[11] VOGEL L, SIHLER H, LAMPEL J, *et al*. Retrieval interval mapping: A tool to visualize the impact of the spectral retrieval range on differential optical absorption spectroscopy evaluations[J]. *Atmospheric Measurement Techniques*, 2013, **6**(2): 275-299.

[12] WU Feng-cheng, LI Ang, XIE Pin-hua, *et al*. Emission flux measurement error with a mobile DOAS system and application to NO_x flux observations[J]. *Sensors*, 2017, **17**(2):231.

[13] SONG Fei-hu, XU Chuan-long, WANG Shi-min. UV differential optical absorption method for measuring sulfur content in coal[J]. *Measurement Science and Technology*, 2012, **23**(2): 025501.

[14] LIU Zi-long, SUN Li-gun, GUO Yin, *et al*. The calibration research of DOAS based on spectral optical density[J]. *Spectroscopy and Spectral Analysis*, 2017, **37**(4): 1302-1306.

[15] YAN Huan-huan, LI Xiao-jing, WANG Wei-he, *et al*. Comparison of SO_2 column retrievals from BRD and DOAS algorithms[J]. *Science China-Earth Sciences*, 2017, **60**(9): 1694-1706.

[16] CHAN K L, LING Liu-yi, HARTL A, *et al*. Comparing different light-emitting diodes as light sources for long path differential optical absorption spectroscopy NO_2 and SO_2 measurements[J]. *Chinese Physics B*, 2012, **21**(11): 119301.

[17] ZHANG Yun-gang, SOMESFALEAN G, GUO Wei, *et al*. An optical system for measuring nitric oxide using spectral separation techniques[J]. *Applied Physics B-Lasers and Optics*, 2012, **107**(2): 435-440.